



**HAL**  
open science

# Damage tracking using distributed optic fiber sensors in structures

Sahar Farahbakhsh, Ludovic Chamoin, Martin Poncelet

► **To cite this version:**

Sahar Farahbakhsh, Ludovic Chamoin, Martin Poncelet. Damage tracking using distributed optic fiber sensors in structures. 25e Congrès Français de Mécanique, Aug 2022, Nantes, France. hal-03934311

**HAL Id: hal-03934311**

**<https://hal.science/hal-03934311v1>**

Submitted on 11 Jan 2023

**HAL** is a multi-disciplinary open access archive for the deposit and dissemination of scientific research documents, whether they are published or not. The documents may come from teaching and research institutions in France or abroad, or from public or private research centers.

L'archive ouverte pluridisciplinaire **HAL**, est destinée au dépôt et à la diffusion de documents scientifiques de niveau recherche, publiés ou non, émanant des établissements d'enseignement et de recherche français ou étrangers, des laboratoires publics ou privés.

# Damage tracking using distributed optic fiber sensors in structures

S. FARAHBAKHS<sup>a</sup>, L. CHAMOIN<sup>a,b</sup>, M. PONCELET<sup>a</sup>

a. Université Paris-Saclay, CentraleSupélec, ENS Paris-Saclay, CNRS, LMPS - Laboratoire de Mécanique Paris-Saclay, 91190, Gif-sur-Yvette, France.

b. Institut Universitaire de France (IUF), 1 rue Descartes, 75005 Paris, France  
sahar.farahbakhsh@ens-paris-saclay.fr, ludovic.chamoin@ens-paris-saclay.fr,  
martin.poncelet@ens-paris-saclay.fr

## Résumé :

*La détection précoce de l'endommagement et le suivi de sa progression contribuent à améliorer la sécurité et la durabilité des structures. La capacité à modéliser et simuler ce phénomène, en complément de mesures, facilite le contrôle du système. Différents types de capteurs ont été utilisés dans le cadre de la surveillance de l'état des structures. Parmi eux, les capteurs à fibre optique distribués offrent divers avantages qui en font une option pratique pour la surveillance en temps réel des structures. Ce travail consiste à utiliser des capteurs distribués de déformation, basés sur la rétrodiffusion de Rayleigh et la technologie OFDR, dans des échantillons qui supportent une charge jusqu'à leur point de rupture. Les données recueillies sont ensuite post-traitées dans le cadre de l'erreur en relation de comportement modifiée (mCRE) pour effectuer la mise à jour du modèle d'endommagement et estimer l'état du matériau. Plusieurs modèles d'endommagement sont présentés et comparés, et le modèle le plus adapté est aussi sélectionné au moyen de la mCRE.*

## Abstract :

*Early detection of damage and monitoring helps improving the safety and durability of structures. The ability to model and simulate this phenomenon, along with measurements, facilitates system control. Various sensor types have been used in the context of structural health monitoring. Among them, Distributed Optic Fiber Sensors grant certain benefits which make them a convenient option for real-time monitoring of structures. This work comprises of using distributed strain sensors, based on Rayleigh backscattering and OFDR technology, in samples that bear loading up to their failure point. The collected data are then post-processed in the framework of modified constitutive relation error (mCRE) to perform damage model updating and estimate the material condition. Several damage models are presented and compared, and the most suitable model is also selected using mCRE.*

**Mots clefs : Damage detection, SHM, Inverse problems, Optic fiber sensors, OFDR, Model Selection**

# 1 Introduction

Damage detection, tracking, and modeling are of great importance in today's complex structures. Early detection of damage makes it possible to observe damage progression and prevent critical issues. The ability to model this phenomenon leads to better control of the structure, preventing or delaying its failure and increasing its safety and durability. Distributed Optic Fiber Sensors (DOFS) are a proper and efficient tool for structural health monitoring and damage detection. Recent advances in optic fiber technology now permit temperature and strain sensing with high spatial resolution, leading to real-time and high accuracy measurements inside the material. These sensors are immune to electromagnetic fields and are simple to install on structures or embed in structural material, which brings them a wide variety of use [1]. A common type of DOFS employs Optical Frequency Domain Reflectometry (OFDR) and Rayleigh backscattering to measure strain or temperature alterations along the fiber [2].

In this work, OFDR sensors are implanted in two different material sets to monitor their state and damage advancement through strain measurements. Damage models are presented for both materials. The acquired measurements are then compared to damage model outputs, for model updating purposes, by means of the modified Constitutive Relation Error (mCRE) concept.

Since material behavior and enforced loading are generally the sole source of uncertainty in the models, mCRE formulates a cost function based on the constitutive relation while taking the measurement noise into account. Furthermore, mCRE enables determining the consistence of the model and measurements. It is thus a robust tool for parameter identification and remains valid even when measurements are corrupted, due to a strong mechanical regularization [3]. For each damage model presented in this work, parameters are adjusted by solving an inverse problem that minimizes the mCRE. In addition, the accuracy of each damage model is assessed and discussed with regards to experimental measurements, through the modeling error part of the mCRE functional, so that model selection can be performed.

In the next section of this paper, the principle behind optic fiber sensing is briefly explained. The concept of CRE and mCRE is presented in section 3, and section 4 consists of details about the experiments, including the sample preparations. Model updating and parameter identification are shortly discussed in the final section.

## 2 Optic fiber sensing

There are various technologies of optic fiber sensing, each with its advantages and drawbacks which makes it convenient for some cases and improper for others. In the case of this study, DOFS based on Rayleigh scattering and OFDR technique have been used for strain sensing. These sensors offer an acceptable sensing range (up to 100 meters), providing real time measurements with a spatial resolution of 2.6 millimeters and a sensing resolution of  $1 \mu\epsilon$ .

### 2.1 Rayleigh scattering

Rayleigh scattering corresponds to the interference of light with small inhomogeneities in the medium, that is, inhomogeneities much smaller in size than the wavelength of the traveling light. In optic fibers, these inhomogeneities are the inevitable faults and fluctuations of the refractive index in the fiber core resulting from the manufacturing process. Although considered a disadvantage in optical fiber telecommunications, backscattering is the essential principle behind optic fiber sensors. Due to the Rayleigh scattering, the incident light interferes with a particle. The forward-propagating light loses energy ; thus,

attenuation occurs. Since scattered light propagates in all directions, a fraction of scattered light is necessarily backscattered toward the input of the fiber (Figure 1), where the backscattered light is captured for sensing purposes. Rayleigh scattering does not change the frequency of the light, a matter which helps develop the concept of OFDR sensors.

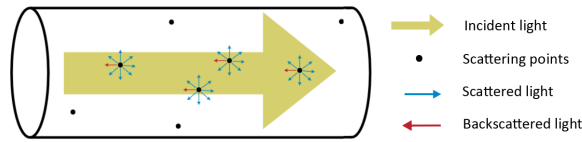


FIGURE 1 – Rayleigh scattering in the fiber core

## 2.2 OFDR sensors

The working principle of these sensors is presented schematically in Figure 2. OFDR sensors use interferometry and a frequency-modulated optical wave [2]. A continuous signal with a linearly swept frequency is produced using a tunable laser source (TLS). The incident light is split into two identical beams, one is sent to a reference arm and the other to the fiber under test (FUT). The backscattered light from these two arms is captured and coupled via a coupler to produce a single signal which is further analyzed by an interferometer. The time delay between the backscattered light from the FUT and the reference light produces a unique beat frequency for each scattering point of the FUT. Moreover, the time delay of the backscattered light corresponds to the light flight time to the scattering point and back. Therefore, each beat frequency can reveal the position of a scattering point on the FUT. These beat frequencies can be obtained by applying a Fourier transform (FFT) to the coupled signal and converting it to the frequency domain. Performing this procedure on the fiber in its reference state, i.e., before applying any temperature or strain changes, provides a unique fingerprint for each fiber. The fingerprint signal, or fiber Rayleigh backscattering signature (RBS), remains the same unless the fiber undergoes an environmental change. Any alteration of temperature or strain causes a slight shift in the position of

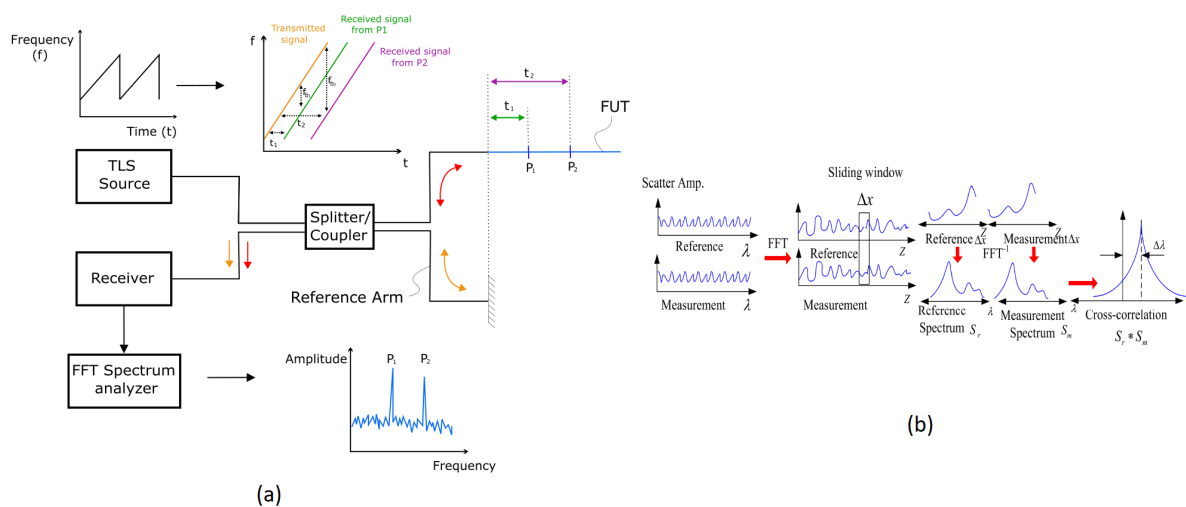


FIGURE 2 – (a) Working concept of OFDR sensors ; (b) Dividing the signal to  $\Delta x$  windows, and cross-correlation (from [1])

the scattering points, which in turn causes a change in the fiber signature. The same procedure is performed on the fiber while experiencing temperature or strain changes. The signature and measurement signals are transferred to spatial domain by performing another FFT, and are both divided into small windows  $\Delta x$ , which indicates the spatial resolution of the method. Each divided part of these two signals, that are captured by the same window  $\Delta x$  in spatial domain, corresponds to the same location on the fiber. For every window  $\Delta x$ , the two divided signals are again transferred into frequency domain via an inverse Fourier transform. Subsequently, two spectra are resulted from each window, which are then cross-correlated. As a result of this cross correlation, a frequency shift appears in the windows where temperature or strain changes have occurred. This shift of frequency is linearly related to the temperature and strain alterations, and the position of the window containing the frequency shift reveals the measurement location [4]. Consequently, this process leads to mapping the temperature or strain measurements throughout the fiber.

### 3 Concept of mCRE

The modified Constitutive Relation Error (mCRE), as is proposed by its name, is developed based on the concept of constitutive relation error (CRE). The CRE functional was primarily introduced for error evaluation in the context of Finite Element method, by presenting an estimation of the discretization error [5]. The idea of CRE energy-based functional is to provide the model error that originates from the model specified constitutive relation, as it is generally the least reliable equation defining the problem compared to two other sets of equations, namely equilibrium and compatibility equations. In more recent applications, CRE was used as a cost function in inverse problems for parameter identification or model updating [6]. In this context, the observations are strongly imposed in the admissibility fields. The CRE functional is minimized in a two-step iterative manner by first finding an admissible displacement-stress couple and then updating the model parameters accordingly. The CRE functional and the minimization problem are presented for a linear elastic case in equations (1) and (2), respectively.

$$\varepsilon_{CRE}^2(\hat{\mathbf{u}}, \hat{\boldsymbol{\sigma}}; \mathbf{p}) = \frac{1}{2} \|\hat{\boldsymbol{\sigma}} - \mathbf{K}(\mathbf{p})\boldsymbol{\epsilon}(\hat{\mathbf{u}})\|_{\mathbf{K}^{-1}}^2 \quad (1)$$

$$\mathbf{p}_{sol} = \operatorname{argmin}_{\mathbf{p} \in \mathcal{P}} \left[ \min_{(\hat{\mathbf{u}}, \hat{\boldsymbol{\sigma}}) \in (\mathbf{A}_d^+)} \varepsilon_{CRE}^2(\hat{\mathbf{u}}, \hat{\boldsymbol{\sigma}}; \mathbf{p}) \right] \quad (2)$$

In these formulations,  $\mathbf{p}$  represents the parameters to be updated, and  $\mathcal{P}$  is the parameter space, whereas  $\hat{\mathbf{u}}$  and  $\hat{\boldsymbol{\sigma}}$  show displacement and stress from kinematic and static admissible search spaces respectively.  $\mathbf{A}_d^+$  is the ensemble of the admissibility space enriched by the observations, hence the plus sign.  $\boldsymbol{\epsilon}(\hat{\mathbf{u}})$  is the strain corresponding to the displacement  $\hat{\mathbf{u}}$ , and  $\mathbf{K}(\mathbf{p})$  stands for the constitutive relation of the problem whose parameters are to be updated.

The advantage of using the CRE functional in inverse problems is that the defined cost function has a physical and mechanical sense. However, enforcing the measurement data directly into the admissible fields as additional constraints can decrease the accuracy of the optimal solution as the measurements always contain a level of noise, and might sometimes be corrupted.

On the other hand, the modified version of the CRE functional, or the mCRE, solves this problem by separating the information into two sets. Reliable information, such as equilibrium equations, known boundary conditions, and sensor locations, is strongly imposed in the admissibility space. On the contrary,

less reliable information, notably constitutive relations, noisy measurements, and unknown boundary conditions, is relaxed [7].

### 3.1 Linear mCRE

Considering the same linear elastic case when the observations are displacements in a subdomain of the structure, the mCRE functional and the following optimization problem are defined by :

$$\varepsilon_{mCRE}^2(\hat{\mathbf{u}}, \hat{\boldsymbol{\sigma}}; \mathbf{p}) = \varepsilon_{CRE}^2(\hat{\mathbf{u}}, \hat{\boldsymbol{\sigma}}; \mathbf{p}) + \frac{\alpha}{2} (\mathbf{d}(\hat{\mathbf{u}}) - \mathbf{d}_{obs})^T \mathbb{G}_{obs}^{-1} (\mathbf{d}(\hat{\mathbf{u}}) - \mathbf{d}_{obs}) \quad (3)$$

$$\mathbf{p}_{sol} = \underset{\mathbf{p} \in \mathcal{P}}{\operatorname{argmin}} \left[ \min_{(\hat{\mathbf{u}}, \hat{\boldsymbol{\sigma}}) \in (\mathbf{A}_d^-)} \varepsilon_{mCRE}^2(\hat{\mathbf{u}}, \hat{\boldsymbol{\sigma}}; \mathbf{p}) \right] \quad (4)$$

Here,  $\varepsilon_{CRE}$  is the same functional defined in (1), and  $\alpha$  is a scalar factor weighing the measurement part of the functional against the model error part, i.e. the term  $\varepsilon_{CRE}^2$ .  $\mathbf{d}_{obs}$  represents the observations and  $\mathbf{d}(\hat{\mathbf{u}})$  is the displacement  $\hat{\mathbf{u}}$  on the domain corresponding the measurements.  $\mathbb{G}_{obs}$  is a normalized scaling matrix usually diagonal, and  $\mathbf{A}_d^-$  is the ensemble of the relaxed admissibility space, hence the negative sign.

Similar to the minimization of  $\varepsilon_{CRE}^2$ , the optimization process of  $\varepsilon_{mCRE}^2$  is carried out in a two-step iterative manner. The first step of each iteration consists of calculating the optimal admissible fields  $(\hat{\mathbf{u}}^{(n)}, \hat{\boldsymbol{\sigma}}^{(n)})$  through a minimization process. In the second step the functional is minimized regarding the parameters  $\mathbf{p}^{(n)}$  while using the values obtained in the first step for the admissible fields  $(\hat{\mathbf{u}}^{(n)}, \hat{\boldsymbol{\sigma}}^{(n)})$ . The superscript (n) indicates the iteration number.

Equation (3) shows that the given inverse problem can be observed from two different angles. The presented explanation is achieved from a mechanical point of view, where  $\varepsilon_{mCRE}^2$  is interpreted as a modified version of  $\varepsilon_{CRE}^2$  with more relaxed constraints to avoid strongly imposing the measurement error into the formulation. Furthermore, from an optimization perspective the  $\varepsilon_{mCRE}^2$  can be perceived as a least squares problem  $[(\mathbf{d}(\hat{\mathbf{u}}) - \mathbf{d}_{obs})^T \mathbb{G}_{obs}^{-1} (\mathbf{d}(\hat{\mathbf{u}}) - \mathbf{d}_{obs})]$  with a mechanical regularization term  $\varepsilon_{CRE}^2$  and regularization parameter  $1/\alpha$ , improving the cost function convexity.

In either approach the  $\varepsilon_{mCRE}^2$  formulation is in fact a compromise between model and measurement data, and the value of  $\alpha$  demonstrates the confidence level in the information. When  $\alpha \rightarrow 0$ , the inverse problem is almost equivalent to the minimization of the  $\varepsilon_{CRE}^2$  with no regard to the measurement information, indicating high measurement uncertainty. Increasing  $\alpha$  implies an increase in confidence towards the measurements. In the extreme case when  $\alpha \rightarrow \infty$ , the inverse problem turns into a classical least squares optimization, with high confidence in measurement data and low confidence in model definition. As  $\alpha$  plays an important role in the quality of the optimization procedure, its value is set based on a priori knowledge of the problem, using Morozov principle in this case [8].

### 3.2 Nonlinear mCRE

Extending this concept to a nonlinear framework with elasto-plastic behavior yields a more complex formulation of mCRE. This generalized case is presented through equations (5) to (8), for a time interval  $[0, T]$  and a structure volume  $\Omega$ .

$$\varepsilon_{CRE}^2(\hat{\mathbf{e}}_e, \hat{\mathbf{e}}_p, \hat{\mathbf{s}}; \mathbf{p}) = \int_0^T \int_{\Omega} \left( \eta_{\psi}(\hat{\mathbf{e}}_e, \hat{\mathbf{s}}; \mathbf{p}) + \int_0^t \eta_{\varphi}(\dot{\hat{\mathbf{e}}}_p, \hat{\mathbf{s}}; \mathbf{p}) \right) \quad (5)$$

$$\eta_\psi(\hat{\mathbf{e}}_e, \hat{\mathbf{s}}) = \psi(\hat{\mathbf{e}}_e) + \psi^*(\hat{\mathbf{s}}) - \hat{\mathbf{s}} \cdot \hat{\mathbf{e}}_e \geq 0 \quad ; \quad \eta_\varphi(\dot{\hat{\mathbf{e}}}_p, \hat{\mathbf{s}}) = \varphi(\dot{\hat{\mathbf{e}}}_p) + \varphi^*(\hat{\mathbf{s}}) - \hat{\mathbf{s}} \cdot \dot{\hat{\mathbf{e}}}_p \geq 0 \quad (6)$$

$$\varepsilon_{mCRE}^2(\hat{\mathbf{e}}_e, \hat{\mathbf{e}}_p, \hat{\mathbf{s}}; \mathbf{p}) = \varepsilon_{CRE}^2(\hat{\mathbf{e}}_e, \hat{\mathbf{e}}_p, \hat{\mathbf{s}}; \mathbf{p}) + \frac{\alpha}{2} \cdot \frac{1}{N_t} \sum_{n_t=1}^{N_t} (\mathbf{d}(\hat{\mathbf{u}}^{n_t}) - \mathbf{d}_{obs}^{n_t})^T \mathbb{G}_{obs}^{-1} (\mathbf{d}(\hat{\mathbf{u}}^{n_t}) - \mathbf{d}_{obs}^{n_t}) \quad (7)$$

$$\mathbf{p}_{sol} = \underset{\mathbf{p} \in \mathcal{P}}{\operatorname{argmin}} \left[ \min_{(\hat{\mathbf{e}}_e, \hat{\mathbf{e}}_p, \hat{\mathbf{s}}) \in (\mathbf{A}_d^-)} \varepsilon_{mCRE}^2(\hat{\mathbf{e}}_e, \hat{\mathbf{e}}_p, \hat{\mathbf{s}}; \mathbf{p}) \right] \quad (8)$$

In these equations,  $\hat{\mathbf{e}}_e$  and  $\hat{\mathbf{e}}_p$  are global flux variables regarding elastic and plastic strains.  $\hat{\mathbf{s}}$  stands for global thermodynamic forces with respect to  $(\hat{\sigma})$ .  $\psi$  and  $\varphi$  denote free energy and dissipation potential, while the dual potentials are shown by  $\psi^*$  and  $\varphi^*$ .  $\eta_\psi$  and  $\eta_\varphi$  respectively represent residuals on state equations and evolution laws,  $\mathbf{a} \cdot \mathbf{b}$  corresponds to duality product of  $\mathbf{a}$  and  $\mathbf{b}$ , and  $N_t$  stands for number of time points. The optimization algorithm is similar to the linear elastic case, as shown in equation (8). Detailed discussion on the nonlinear mCRE can be found in references [9] and [10].

## 4 Experiments

In a first attempt, a cement-based fiber-reinforced mortar is used for beam samples to ensure nearly homogenous, isotropic and nonfragile behavior. A single optic fiber sensor passes through the beam sample several times to provide measurements in different points of the beam section. A second type of sample is also prepared consisting in a fiber reinforced polymer plate. An optic fiber sensor is embedded inside the plate to monitor its damage during the tests.

Both sets of samples undergo a quasi-static 4-point bending test (Figure 3). This arrangement provides an uniform pure-bending state in the beam sector between loading pins A and B. A few cycles of quasi-static loading and unloading are applied within the elastic limit of the material. In the final cycle, loading is increased until the rupture of the sample.

### 4.1 Concrete samples

The cement-based mortar is reinforced with polyamide and steel fibers to increase the ductility as well as the tensile strength of the concrete. The state of this material is isotropic and homogenous along the beam axis ( $z$ ). However, as these samples undergo a 4-point bending test, the behavior of material along the height of the beam ( $y$ -axis) starts as homogenous, elastic and linear; then turns heterogenous with the appearance and progression of cracks in the concrete.

The optic fiber sensor is crossed through both parts of the beam that are under tension and compression. Dimensions of the sample and placement of the fiber in the beam section are presented in Figure 3.

### 4.2 Composite samples

The second material set is a composite with carbon fiber reinforcements pre-impregnated by epoxy. This composite plate consists of 8 different layers with a quasi-isotropic stacking, leading to a homogenous characteristic at macroscale. However, it is considered heterogenous and anisotropic at microscale. The sensor is passed through the composite mid-layer. The chosen orientation of the layers and the placement of the sensor are shown in Figure 4.

Since the fiber is positioned at the mid-layer of the composite, in a bending test it falls on the plate

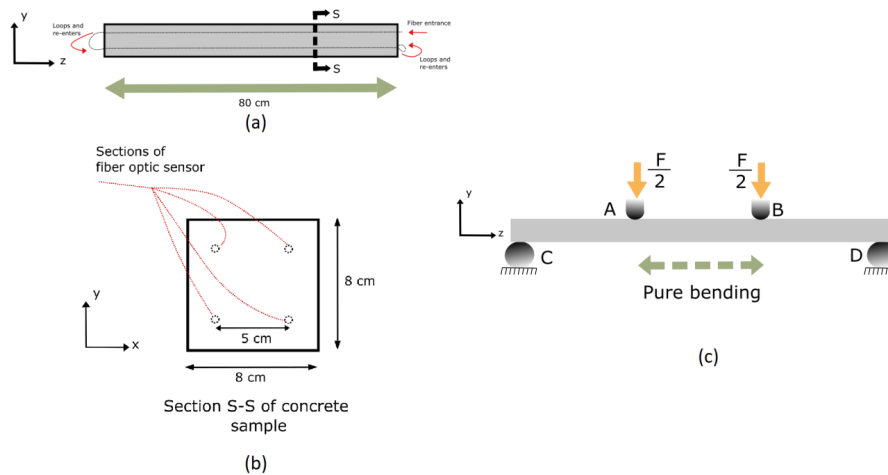


FIGURE 3 – (a) and (b) Dimensions of concrete sample and positioning of embedded fiber ; (c) Schematic set-up of a 4-point bending test

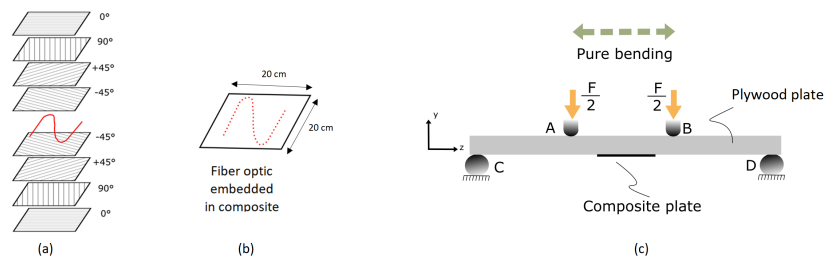


FIGURE 4 – (a) Composite layout. The angles show the orientation of carbon fibers in each layer; (b) Optic fiber placement in the composite plate; (c) 4-Point bending test set-up for composite samples glued to wooden plates

neutral axis where no strain is expected. To resolve this issue, the composite is as aforementioned glued on the bottom of a thicker plywood plate, and the assemblage is installed on the bending test machine. Therefore, the composite plate bears the maximum tension resulted from bending of the assemblage (Figure 4).

## 5 Model updating

Real-time data from the tests are exploited in the mCRE formulation for parameter updating in the introduced models. Measurements from each instant of the loading process can be used separately in the formulation to provide information on the state of the sample and the progression of damage, if applicable, at that specific instant.

The data obtained from loading and unloading cycles within the elastic limit of the material are used to identify and update undamaged model parameters, e.g. the correct initial Young modulus of the material. The resulting updated parameters are used in the definition of damage models for each material, and immediately after first signs of damage, those parameters characterizing the state of damage and its progression, are picked to be updated.

In a first approach for each material, a simple isotropic damage model is presented as in (9) where the



state of damage is declared by a local decrease in the Young modulus.

$$E_d = E(1 - d) \quad (9)$$

Here,  $E_d$  is the reduced Young modulus, indicating damage has occurred.  $d$  is the damage parameter to be updated and  $E$  is the initial Young modulus of the material, before it is damaged. The value of  $E$  is determined by parameter updating during the elastic phase of the loading cycles, as previously explained.

Moreover, a more sophisticated and orthotropic damage model is presented where three damage parameters are used to better estimate the damage state of the structure. As for the progression of damage, several models based on different evolution equations are implemented in addition to state equations. Identification and updating the parameters in these models lead to the prediction of the damage state, or in other words, defining the damage progression. The attained functionals and determined damage localizations are compared to perform model selection.

This project has received funding from the European Research Council (ERC) under the European Union's Horizon 2020 research and innovation program (grant agreement No. 101002857).

## Références

- [1] Z. Ding, C. Wang, K. Liu, J. Jiang, D. Yang, G. Pan, Z. Pu, and T. Liu, "Distributed optical fiber sensors based on optical frequency domain reflectometry : A review," *Sensors*, vol. 18, no. 4, p. 1072, 2018.
- [2] X. Bao and Y. Wang, "Recent advancements in rayleigh scattering-based distributed fiber sensors," *Advanced Devices & Instrumentation*, vol. 2021, 2021.
- [3] O. Allix, P. Feissel, and H. Minh Nguyen, "Identification strategy in the presence of corrupted measurements," *Engineering Computations*, vol. 22, pp. 487–504, 2005.
- [4] X. Bao and L. Chen, "Recent progress in distributed fiber optic sensors," *Sensors*, vol. 12, no. 7, pp. 8601–8639, 2012.
- [5] L. Chamoin and P. Ladevèze, "The Constitutive Relation Error method : a general verification tool," in *Verifying calculations – forty years on* (L. Chamoin and P. Diez, eds.), Springer, 2016.
- [6] R. V. Kohn and B. D. Lowe, "A variational method for parameter identification," *ESAIM : Mathematical Modelling and Numerical Analysis - Modélisation Mathématique et Analyse Numérique*, vol. 22, no. 1, pp. 119–158, 1988.
- [7] P. Ladevèze and A. Chouaki, "Application of a posteriori error estimation for structural model updating," *Inverse problems*, vol. 15, no. 1, p. 49, 1999.
- [8] V. A. Morozov, "The error principle in the solution of operational equations by the regularization method," *Ussr Computational Mathematics and Mathematical Physics*, vol. 8, pp. 63–87, 1968.
- [9] P. Ladevèze and N. Moës, "A new a posteriori error estimation for nonlinear time-dependent finite element analysis," *Computer Methods in Applied Mechanics and Engineering*, vol. 157, no. 1 2, pp. 45–68, 1998.
- [10] B. Marchand, L. Chamoin, and C. Rey, "Parameter identification and model updating in the context of nonlinear mechanical behaviors using a unified formulation of the modified constitutive relation error concept," *Computer Methods in Applied Mechanics and Engineering*, vol. 345, pp. 1094–1113, 2019.